

Damage Modeling of Degradable Polymers Under Bulk Erosion

C. Y. Tang,¹ Z. W. Wang,² C. P. Tsui,¹ Y. F. Bai,¹ B. Gao,³ H. Wu⁴

¹Department of Industrial and Systems Engineering, The Hong Kong Polytechnic University, Hung Hom, Kowloon, Hong Kong, People's Republic of China

²Department of Process Equipment and Control Engineering, Dalian University of Technology, Dalian 116012, People's Republic of China

³Department of Prosthodontics, Qin Du Stomatological Hospital, the Fourth Military Medical University, Xi'an 710032, People's Republic of China

⁴Department of Pharmaceutical Chemistry, The Fourth Military Medical University, Xi'an 710032, People's Republic of China

Correspondence to: C. P. Tsui (E-mail: mfgary@inet.polyu.edu.hk)

ABSTRACT: Unit micro-cell models with different architectures were designed to simulate the degradation process and chemical damage behavior of degradable polymers under bulk erosion. The pores in the micro-cell models were introduced to mimic the state of rapid water diffusion into the polymers under bulk erosion, while three different arrangements of pores were considered to investigate their effects on the degradation rate of different polymers with the same molecular weight. Different porosity levels were also used to study the degradation responses of the polymers having different molecular weights. A heat and mass transfer analogy was adopted to enable the analysis to be run on a general purpose finite element (FE) code. In the present work, a finite element software package ABAQUS incorporated with a user-defined material subroutine was used to perform the analysis, in which a heat transfer function was utilized to simulate Fickian mass diffusion for the polymers through analogy. With the proposed method, the effects of chemical damage on the mechanical properties of the degradable polymers under bulk erosion could be predicted and the predicted trend of the mass loss of the polymers followed experimental results obtained from the open literature. © 2012 Wiley Periodicals, Inc. *J. Appl. Polym. Sci.* 000: 000–000, 2012

KEYWORDS: biopolymers and renewable polymers; computer modeling; degradation

Received 24 August 2011; accepted 25 July 2012; published online

DOI: 10.1002/app.38404

INTRODUCTION

For bone reconstruction, a degradable polymer-based scaffold is expected to restore the mechanical strength temporarily, and support and guide new bone tissue ingrowth.¹ During the course of the polymer degradation, the polymer backbone chains are broken into oligomers and eventually monomers due to hydrolysis. The extensive degradation of the polymer causes erosion and mass loss due to the substantial scission of its chains.^{2–5} Polymers such as poly(glycolic acid) (PGA) and poly(lactic acid) (PLA) are usually degraded by bulk erosion due to rapid water uptake followed by hydrolysis of the ester bonds,^{2,6} which leads to a reduction in their molecular weight. Many models based on diffusion-reaction equations have been developed mainly to describe the water-dependent degradation process and mass loss for bulk eroding polymers,^{3–5,7} rather than their mechanical strength degradation. A mathematical model combining stochastic hydrolysis and the diffusion-reaction process has also been developed to predict the degradation for bulk eroding polymers.^{8,9}

Biodegradable porous polymer structures have several advantages in bone tissue engineering; however, mechanical failure of a repair often occurs^{10–12} when degrading polymers transfer their load-bearing duty to the developing tissue prior to sufficient ingrowth and remodeling. Therefore, it is important to predict the mechanical property degeneration rate of the implant, especially the polymer matrix. Although the bulk erosion of polymers has been studied extensively, relatively limited work¹³ has been reported on quantitatively investigating the mechanical strength degradation of bulk eroding polymers with respect to time. A method which can predict the gradual degeneration of mechanical properties of polymers with different degradation rates is important for the design of degradable structures for bioapplications.

As the principles of mass transfer and heat transfer are similar, a heat and mass transfer analogy has been successfully applied in the prediction of various phenomena, such as mass diffusion in materials and passive cooling in light water nuclear

reactors.^{14,15} Moreover, the finite element method (FEM) has been applied to simulate the diffusional mass transport and chemical reaction processes in polymers through this analogy.¹⁶ Although commercially available FEM software packages such as ABAQUS have been widely used for modeling the mechanical and damage behavior of polymer-based composites and bio-composites,^{17–19} the mass transfer subroutine for predicting the polymer degradation is not always available. In view of this, the present work was to apply the heat and mass transfer analogy so that the heat transfer function in the FE software package could be used to simulate Fickian mass diffusion for the polymers under bulk erosion. Moreover, the application of this analogy, together with the present finite element cell modeling approach, could be utilized to predict not only the polymer degradation but also the effect of degradation on the mechanical properties of the bulk eroding polymers. In the present work, the degradation process and chemical damage behavior of degradable polymers under bulk erosion were predicted by using three different unit micro-cell models in an ABAQUS finite element code coupled with the heat and mass transfer analogy. Moreover, it would enable the effects of varying the porosity levels of the micro-cell models on the degradation behavior, as well as the effects of the chemical damage on the mechanical property of the polymers to be predicted.

METHOD AND IMPLEMENTATION

To simulate the degradation process and chemical damage behavior of degradable polymers under bulk erosion, unit micro-cell models with three different architectures serving as the representative volume elements (RVEs) were designed. A flowchart of the modeling approach is shown in Figure 1. The three different architectures include a face-centered-cubic arrangement of spherical pores with corner pores, a regular packing of cubic pores and a face-centered cubic arrangement of spherical pores without corner pores, denoted as Model A, B, C, respectively, as shown in Figure 2(a–c). The pores in Figure 2 were used to show the main void region in the micro-cell models, and created to mimic the diffusion of water into the polymer quickly so as to ensure that the degradable polymer could undergo degradation due to bulk erosion. The different architectures of the micro-cell models were used to investigate the degradation rate of different degradable polymers with the same molecular weight, while different porosity levels, 8.6, 35.2, 60.8, and 85.6%, were also used in the study with different molecular weight under bulk erosion for 26 weeks.

To simulate the degradation of the polymer, only one-eighth of the unit micro-cell model for each porosity level was considered and a periodic boundary condition was applied due to the symmetry, such that all the surfaces normal to the x , y , and z axes except its upper surfaces, were fixed as shown in Figure 2(d). To ensure a high level of numerical accuracy, the micro-cell models were discretized into 60,000–80,000 three-dimensional four-node linear tetrahedron (DC3D4) elements.

The micro-cell models were considered to be immersed in a water solution with a concentration, c_w of 1 g cm⁻³ at an ambient temperature of 36.5°C, and the initial solution concentra-

tion in the models was set to zero. For each micro-cell model, a normal stress of 0.95 MPa, which was about 50% of the tensile strength of the polymer, was applied onto its upper surfaces perpendicular to the y -direction to determine the displacement. Then, the nominal strain of the micro-cell model was calculated through dividing the determined displacement by the original cell length. Hence, the Young's modulus of the micro-cell model was determined by calculating the ratio of the prescribed nominal stress to the nominal strain at different time period. Reader can obtain more details for determining the Young's modulus by referring to our previous work.^{17,19}

Heat and Mass Transfer Analogy

The heat conduction of a material is governed by Fourier's law,^{20,21}

$$q = -k\nabla\theta \quad (1)$$

where θ and q are the temperature (K) and the heat flux (W m⁻²), respectively; ∇ is the gradient operator; and k is the thermal conductivity (W m⁻¹ K⁻¹) for fully isotropic thermal diffusion.

Assuming no internal heat generation, the governing equation of heat transfer yielded by the energy balance may be described as

$$\rho c_s \frac{\partial\theta}{\partial\tau} + \nabla \cdot q = 0 \quad (2)$$

where τ is the time, ρ and c_s are the density (kg m⁻³) and the specific heat (J kg⁻¹ K⁻¹) of the material, respectively.

With the assumption of uniform thermal conductivity, eqs. (1) and (2) yield the following thermal conduction equation

$$\frac{\partial\theta}{\partial\tau} = \alpha\nabla^2\theta \quad (3)$$

Where ∇^2 is the Laplace operator ($\frac{\partial^2}{\partial x^2} + \frac{\partial^2}{\partial y^2} + \frac{\partial^2}{\partial z^2}$), α is the thermal diffusivity (m² s⁻¹) of the material such that $\alpha = \frac{k}{\rho c_s}$.

The concentration change of a material in mass diffusion is governed by Fick's first law^{22,23} as

$$J = -D\nabla c \quad (4)$$

where c and J express the concentration (kg m⁻³) and the mass flux (kg m⁻² s⁻¹), respectively; D is the diffusion coefficient (m² s⁻¹) of an isotropic diffusion material, such that D is equal to 4.63 × 10⁻¹¹ cm² s⁻¹ for degradable polymers in Ref. 24.

Assuming no substance generation, the solution diffusion yielded by the mass conservation can be calculated with Fick's second law,

$$\frac{\partial c}{\partial\tau} + \nabla \cdot J = 0 \quad (5)$$

Combining eqs. (4) and (5) yields the following mass diffusion equation

$$\frac{\partial c}{\partial\tau} = D\nabla^2 c \quad (6)$$

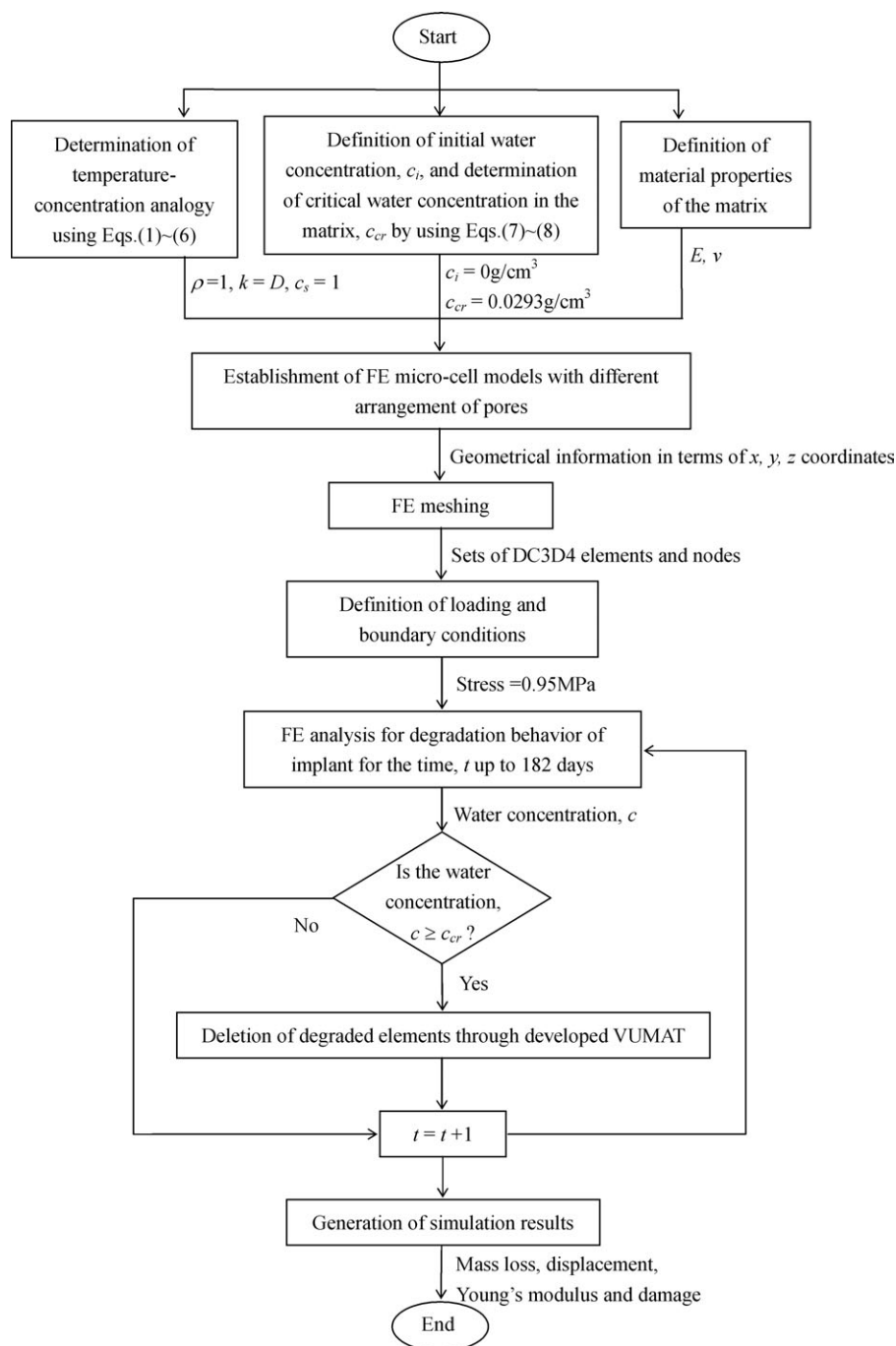


Figure 1. Flowchart of numerical procedure.

The heat and mass transfer analogy was established by a direct comparison of eqs. (3) and (6), and the parameters used in the analogy scheme are summarized in Table I. As eqs. (3) and (6) were derived on the basis of the assumption of uniform thermal conduction and mass diffusion, this analogy is valid only when the diffusion is uniform within the diffusing medium.

Model for Chemical Damage due to Bulk Erosion

In this study, the degradable polymer was assumed to undergo bulk erosion and degrade due to the chemical reaction of the polyesters, given by $\text{—COO—} + \text{H}_2\text{O} \rightarrow \text{—COOH} + \text{HO—}$.²⁵

Therefore, the decreasing rate in the molecular weight of the polymer, M_w , was simply assumed to be related to the local water concentration c ($0 < c < 1$),

$$\frac{dM_w}{dt} = -\beta c \quad (7)$$

where the coefficient β was assumed to be 4000 day^{-1} .²⁶

Moreover, the chemical reaction kinetics of ester bonds in degradable polymers such as PGA and PLA is usually first-order,¹

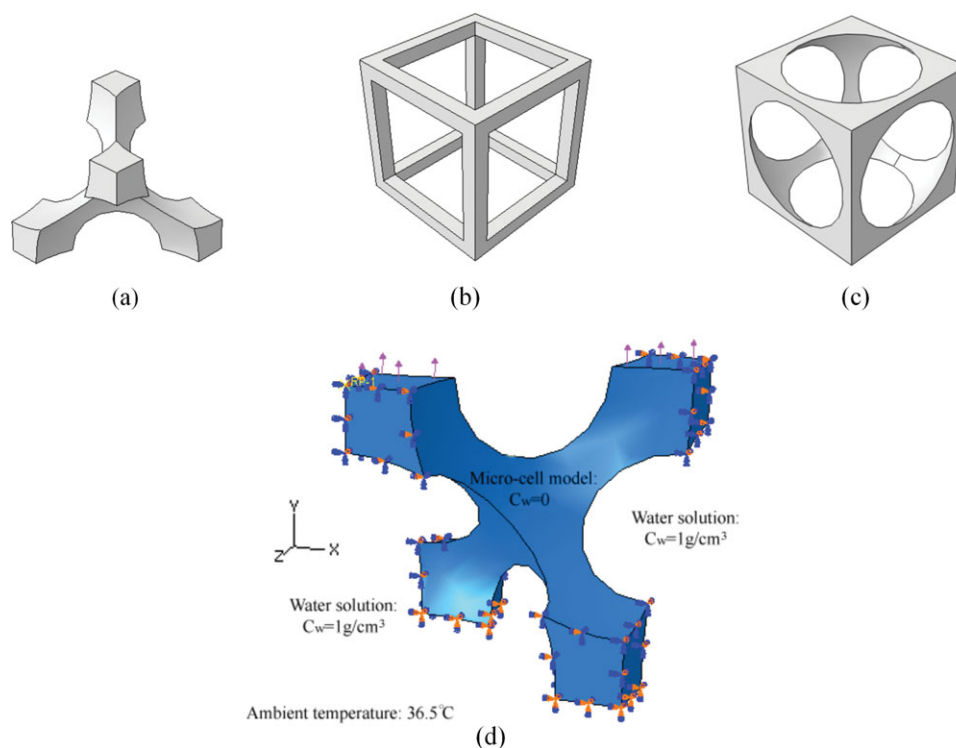


Figure 2. Micro-cell models with porosity of 85.6%, (a) Model A, (b) Model B, (c) Model C, and (d) loading and boundary conditions of Model A. [Color figure can be viewed in the online issue, which is available at wileyonlinelibrary.com.]

$$\frac{dM_w}{dt} = -\lambda M_w \quad (8)$$

where M_w is the average molecular weight of the polymer and λ is the degradation rate constant of the polymer, which depends on the pH condition, temperature and drug load, and the value $\lambda = 0.0117 \text{ day}^{-1}$ was taken from the literature.²⁵

When a degradable polymer is subjected to bulk erosion, its average molecular weight, M_w would decrease. When M_w is lower than the critical average molecular weight $M_{cr} = 10,000 \text{ Da}$,²⁶ there is a chemical damage in the polymer. By using the value of M_{cr} , together with eqs. (7) and (8), the critical water concentration, c_{cr} for the occurrence of chemical damage in each element was found to be 0.0293 g cm^{-3} . When the value of c is equal to or greater than that of c_{cr} , chemical damage of the polymer is assumed to occur. After the initiation of the chemical damage, the degraded elements in the finite element micro-cell model of the polymer are converted into an inactive state and deleted through an element vanishing technique, incorporated into the developed user subroutine VUMAT in ABAQUS.²⁷ Moreover, the initial Young's modulus and Poisson's ratio for the bulk eroding polymer were assumed to be equal to 1570 and 0.39 MPa, respectively.²⁶

RESULTS AND DISCUSSION

Effects of Different Architectures of the Micro-Cell Model on the Degradation Behavior

The micro-cell models with different architectures and the same porosity level of 85.6% have been used to simulate the effects of varying model structure on the degradation behavior of degrad-

able polymers with the same molecular weight under bulk erosion. The simulated results are shown in Figure 3. The micro-cell models were initially at an intact state as shown in Figure 2(a–c). Because of a water concentration gradient between the boundaries and the central region of the micro-cell models, water molecules could rapidly diffuse into the models, as shown in Figure 3(ai–ci), but the water concentration in these micro-cell models did not reach the critical level before the 4th week. Excessive inflow of water molecules could lead to polymer chain scission and consequently a reduction in its molecular weight in three different micro-cell models. When any elements in the micro-cell models reached the critical water concentration, the degraded elements were removed, leading to the increase in the pore size of the micro-cell models under bulk erosion [Figure 3(aii–cii)]. For each of the models, the polymer failure was regarded to occur when any strut of the model was broken due to an excessive number of degraded elements after a certain period of degradation time, as shown in Figure 3(aiii–ciiii).

Figure 4 shows the evolution of the percentage of mass loss for the three different micro-cell models illustrated in Figure 3. It

Table I. Parameters of the Heat and Mass Transfer Analogy Scheme

	Heat transfer	Mass diffusion
Field variable	Temperature, θ	Concentration, c
Density	ρ	1
Conductivity/diffusivity	k	D
Specific heat	c_s	1

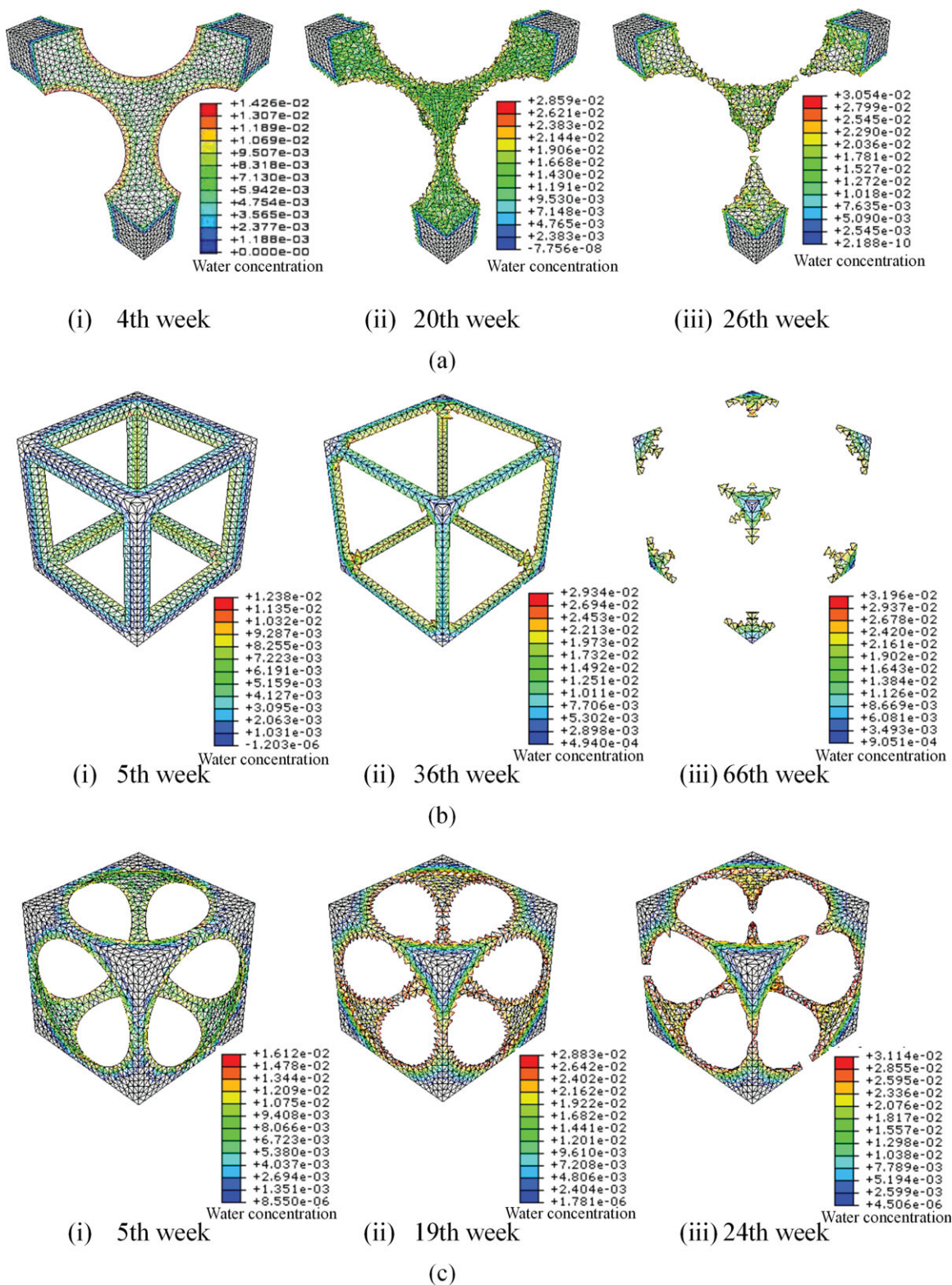


Figure 3. Degradation processes of the three micro-cell models with porosity of 85.6% in terms of water concentration, (a) Model A, (b) Model B, and (c) Model C. [Color figure can be viewed in the online issue, which is available at wileyonlinelibrary.com.]

can be observed that the mass of all the cell models remained almost unchanged up to the 4th week, beyond which there was a mass loss due to increasing number of degraded elements. In

addition, the failure of model B due to the polymer failure occurred in the 66th week, which was much later than those of model A (26th week) and model C (24th week). It is because, for

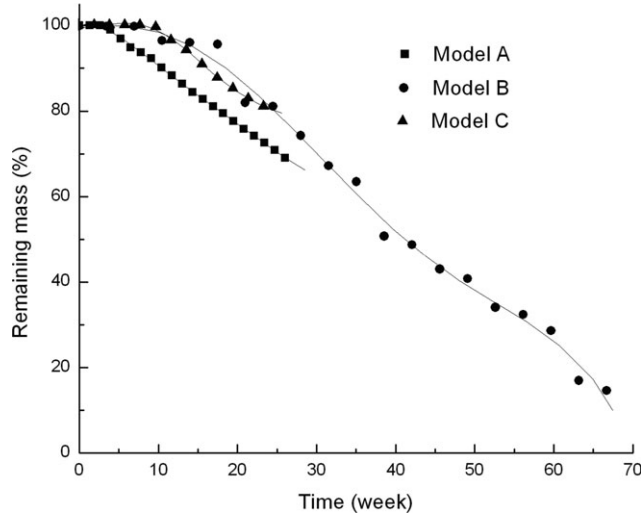


Figure 4. Percentage of mass loss for the three micro-cell models with porosity of 85.6%.

the same porosity level, model C with higher surface area facilitated the water diffusion, leading to a higher degradation rate than model B and its earlier polymer failure at the 24th week. Moreover, from the perspective of the micro-architecture of the models, models A and C did not have uniform strut thickness unlike model B. Therefore, the earlier failure of models A and C could be attributed to the fact that the thinnest regions of these two models failed much faster than the other regions, where the critical water concentration was not yet reached.

Effects of Varying Porosity Levels on Degradation Rates

Micro-cell models with varying porosity levels have been used to simulate the degradation behavior of degradable polymers with different molecular weight under bulk erosion. The mass loss of the three different micro-cell models with different porosity levels, and the experimental data of PLGA²⁸ undergoing bulk erosion²⁹ are shown in Figure 5. It can be seen that, for each of the studied micro-cell models, a higher porosity level and hence a lower molecular weight resulted in an earlier occurrence of degradation, and a high degradation rate and hence the mass loss rate.

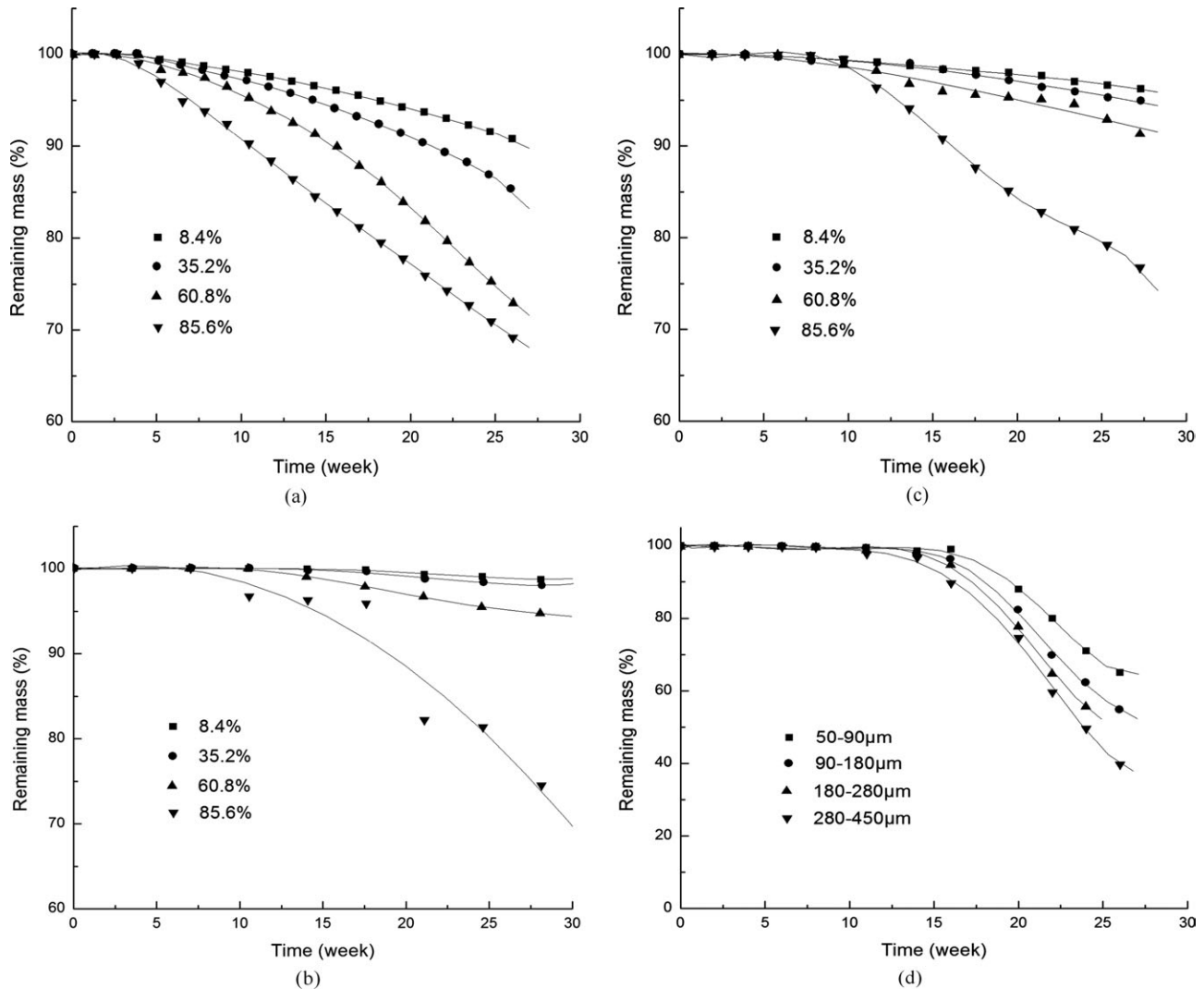


Figure 5. Mass loss versus time for the three micro-cell models with different porosities, (a) Model A, (b) Model B, (c) Model C, and (d) experimental data from Ref. 28.

It is because, for the micro-cell model with a higher porosity level and hence thinner strut, the water concentration in each element can more easily reach the critical concentration, which leads to the earlier initiation of the degradation. The predicted results, as shown in Figure 5(a–c), follow a similar trend for the experimental data as shown in Figure 5(d), such that the mass loss rate of the models with a higher porosity level are higher after the initiation of the polymer degradation.

Effect of Chemical Damage on Mechanical Property

Variations of the strain, Young's modulus and the damage variable predicted by the three micro-cell models, with porosity of 85.6%, versus time are shown in Figure 6. It can be observed from Figure 6(a) that the change in strain of models A and C under the applied loading was generally higher than that of model B up to the 24th week. The difference in the slope of the curves became significant beyond the 10th week, leading to a sharper decrease of Young's moduli of models A and C after this time, as shown in Figure 6(b). According to damage mechanics theory,³⁰ the damage variable, d is defined on the basis of a RVE. The micro-cell model was chosen as the RVE for defining the damage variable d in terms of the apparent Young's modulus of the polymer due to the chemical damage at the unit cell level

$$d = 1 - \frac{E}{E_0} \quad (9)$$

where E_0 is the initial (undamaged) Young's modulus of the polymer, while E is the apparent Young's modulus as a result of the bulk erosion determined by the micro-cell models. The value of d against time can be used for representing the damage evolution of the polymer under bulk erosion. Figure 6(c) shows the damage evolution of the polymer under bulk erosion predicted by different micro-cell models. At the time zero, each model was initially intact and hence its damage value d was zero until the 4th week, for all the models. Beyond the 4th week, model A started to initiate chemical damage and hence its damage variable started to increase. From Figure 6(c), the maximum values of d are 0.71, 0.68, and 0.59 for models A, B and C, respectively, at the moment of polymer failure. Models A and C show higher damage evolution rates and predict the occurrence of material failure at a similar time. As model B has a lower damage evolution rate, material failure does not occur up to the 66th week and the maximum d value of model B is less than that of model A.

Discussion on Importance of Simulating the Degradation

The mechanical stiffness and strength are two key factors for scaffold tissue engineering. Adachi et al.¹ conducted a finite element simulation for scaffold degradation and bone tissue regeneration in a scaffold–bone system. It was demonstrated that the tissue ingrowth has to match with degradation rate of the scaffold material; otherwise the formation of new bone could not have sufficient load-bearing capacity when the scaffold has lost its original topology and its mechanical function has been transferred to the bone. Moreover, Chen et al.⁹ modeled the degradation process and tissue in-growth through a stochastic hydrolysis degradation model and a mechano-regulatory tissue regeneration model, respectively. It was found that a balance between the mechanical stiffness and the porosity level of the scaffolds is important for

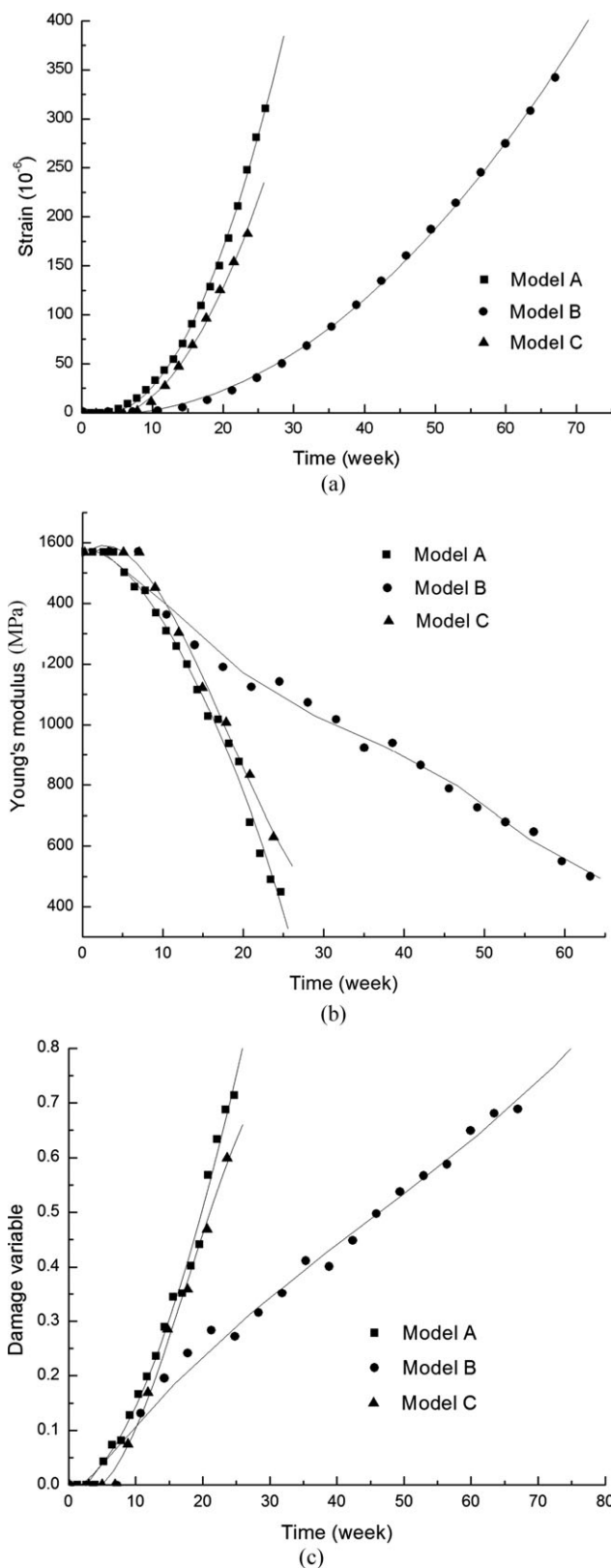


Figure 6. Variation of (a) strain, (b) Young's modulus, and (c) damage d of the three micro-cell models with time.

the load-bearing capacity and permeability of the scaffold–tissue system. Furthermore, van Tienen et al.³¹ conducted *in vivo* tissue ingrowth and *in vitro* degradation of a biodegradable porous polymer scaffold for a knee meniscus defect. The scaffold was found to be unsuitable for the meniscus reconstruction because the tissue ingrowth could not be fully achieved before the initiation of the polymer degradation and the stiffness of the scaffold was also inadequate. In all, it is important to have a correct prediction for the damage rate of degradable polymers for the optimal design of degradable scaffolds with required mechanical properties to support tissue ingrowth. In this article, a new predictive approach is developed based on the micro-cell models and the heat and mass transfer analogy, by which the degradation behavior of the bulk-eroding polymers can be simulated. Moreover, the stiffness of the polymer during the degradation process can also be determined by the micro-cell model using FEM. With the concept of damage mechanics, the material damage of the degradable polymer can be calculated and represented by the damage variable. Therefore, this work contributes a new approach and provides a method for designing new polymeric scaffolds with a balance between the implant degradation and the tissue ingrowth rates.

CONCLUSION

A balance between tissue ingrowth rate and the degradation rate of polymer scaffolds is important for a successful bone reconstruction. Otherwise, scaffold failure may occur before the bone tissue regeneration. In this study, a finite element (FE) approach with a heat and mass transfer analogy has been developed to predict the degradation process and chemical damage behavior of degradable polymers under bulk erosion. Three micro-cell models having different architectures have been effective in simulating the polymers producing different degradation behavior. Model B was found to be suitable for modeling the similar-molecular-weight polymers with a slower degradation rate. The results showed that, after 14 weeks, the mass of the micro-cell models gradually decreased due to a hydrolyzed effect. The effects of varying the porosity levels on the degradation behavior of the micro-cell models with three different architectures have also been predicted. The cell models with lower porosity degraded more slowly than those with higher porosity, and the predicted trend agreed with the experimental results from the open literature. The micro-cell models are also capable of predicting the effect of the chemical damage on the mechanical stiffness of the bulk-eroding polymers, which is important information for the design of scaffolds with the required degradation rate and a mechanical performance to support tissue ingrowth.

ACKNOWLEDGMENTS

The authors are grateful for the substantial support from the Research Grants Council of Hong Kong (PolyU5284/08E) and the Research Committee of the Hong Kong Polytechnic University (G-YG18).

REFERENCES

- Adachi, T.; Osako, Y. K.; Tanaka, M.; Hojo, M.; Hollister, S. J. *Biomaterials* **2006**, *27*, 3964.
- Sckett, C. K.; Narasimhan, B. *Inter. J. Pharm.* **2011**, *418*, 104.
- J. S.; Zunino, P. *Biomaterials* **2010**, *31*, 3032.
- Korber, M. *Pharm. Res.* **2010**, *27*, 2414.
- Rothstein, S. N.; Federspiel, W. J.; Little, S. R. *Biomaterials* **2009**, *30*, 1657.
- Rezwan, K.; Chen, Q. Z.; Blaker, J. J.; Boccaccinia, A. R. *Biomaterials* **2006**, *27*, 3413.
- Thombre, A. G.; Himmelstein, K. J. *AIChE J.* **1985**, *31*, 759.
- Chen, Y. H.; Zhou, S. W.; Li, Q. *Acta Biomater.* **2011**, *7*, 1140.
- Chen, Y. H.; Zhou, S. W.; Li, Q. *Biomaterials* **2011**, *32*, 5003.
- Durselen, L.; Dauner, M.; Hierlemann, H.; Planck, H.; Claes, L. E.; Ignatius, A. J. *Biomed. Mater. Res.* **2001**, *58*, 666.
- Lu, L.; Peter, S. J.; Lyman, M. D.; Lai, H. L.; Leite, S. M.; Tamada, J. A.; Uyama, S.; Vacanti, J. P.; Langer, R.; Mikos, A. G. *Biomaterials* **2000**, *21*, 1837.
- Ferguson, T.; Qu, J. *ASME J. Elect. Packag.* **2002**, *124*, 106.
- Farrar, D. F.; Gillson, R. K. *Biomaterials* **2002**, *23*, 3905.
- Incropera, F. *Fundamentals of Heat and Mass Transfer*; Wiley: New York, **1985**.
- Ambrosini, W.; Forgione, N.; Manfredini, A.; Oriolo, F. *Nuclear Eng. Des.* **2006**, *236*, 1013.
- Wadiak, D. T. *Math. Model.* **1986**, *7*, 385.
- Tsui, C. P.; Tang, C. Y.; Fan, J. P.; Xie, X. L. *Inter. J. Mech. Sci.* **2004**, *46*, 1659.
- Fan, J. P.; Tsui, C. P.; Tang, C. Y.; Chow, C. L. *Biomaterials* **2004**, *25*, 5363.
- Tsui, C. P.; Chen, D. Z.; Tang, C. Y.; Uskokovic, P. S.; Fan, J. P.; Xie, X. L. *Compos. Sci. Technol.* **2006**, *66*, 1521.
- Welty, J. R.; Wicks, C. E.; Wilson, R. E.; Rorrer, G. L. *Fundamentals of Momentum, Heat and Mass Transfer*, 4th ed.; Wiley: New York, **2000**.
- Lykov, A. V.; Mikhailov, Y. A. *Theory of Heat and Mass Transfer*; Israel Program for Scientific Translations: Jerusalem, **1965**.
- Jost, W. *Diffusion in Solids, Liquids, Gases*, 3rd ed.; Academic: New York, **1960**.
- Crank, J. *The Mathematics of Diffusion*, 2nd ed.; Oxford University Press: UK, **1975**.
- Yoon, J. S.; Jung, H. W.; Kim, M. N.; Park, E. S. *J. Appl. Polym. Sci.* **2000**, *7*, 1716.
- Gopferich, A. *Macromolecules* **1997**, *30*, 2598.
- Sanz-Herrera, J. A.; Garcia-Aznar, J. M.; Doblare, M. *Acta Biomater.* **2009**, *5*, 219.
- Zardiackas, L. D.; Parsell, D. E.; Dillon, L. D.; Mitchell, D. W.; Nunnery, L. A.; Poggie, R. J. *Biomed. Mater. Res.* **2001**, *58*, 180.
- Wu, L. B.; Ding, J. D. *J. Biomed. Mater. Res.* **2005**, *75A*, 767.
- von Burkersroda, F.; Schedl, L.; Gopferich, A. *Biomaterials* **2002**, *23*, 4221.
- Lemaitre, J. A. *Course on Damage Mechanics*; Springer: New York, **1992**.
- van Tienen, T. G.; Heijkants, R. G. J. C.; Buma, P.; de Groot, J. H.; Pennings, A. J.; Veth, R. P. H. *Biomaterials* **2002**, *23*, 1731.